EUROPEAN FUSION DEVELOPMENT AGREEMENT

Power Exhaust on JET: An Overview of Dedicated Experiments

W.Fundamenski, P.Andrew, T.Eich[1], G.F.Matthews, R.A.Pitts[2], V.Riccardo, W.Sailer[3], S.Sipila[4] and JET EFDA contributors[5]

Euratom/UKAEA Fusion Association, Culham Science Centre, Abingdon, OX14 3DB, UK
2) CRPP-EPFL, Association Euratom-Confédération Suisse, CH-1015 Lausanne, Switzerland
3) Universität Innsbruck, Technikerstraße 25, A-6020 Innsbruck, Austria
4) Helsinki U. of Technology, Tekes-Euratom Assoc., PO Box 2200, FIN-02015 HUT, Finland
5) See annex to J. Pamela, Fus. Energy 2002 (Proc. 19th Int. Conf. Lyon, 2002), IAEA, Vienna

followed by

Wall and Divertor Load during ELMy H-mode and Disruptions in ASDEX Upgrade

A. Herrmann, J. Neuhauser, G. Pautasso, V. Bobkov, R. Dux, T. Eich, C.J. Fuchs, O. Gruber, C. Maggi, H.W. Müller, V. Rohde, M. Y. Ye, ASDEX Upgrade team[1]

1) Max-Planck-Institut für Plasmaphysik, EURATOM-Association, Boltzmann Str. 2., D-85748, Garching, Germany

Power Exhaust: Outline

- **Steady-state (inter-ELM)**
  - fwd-B
  - rev-B
- **Transient (ELMs)**
  - JET
  - AUG

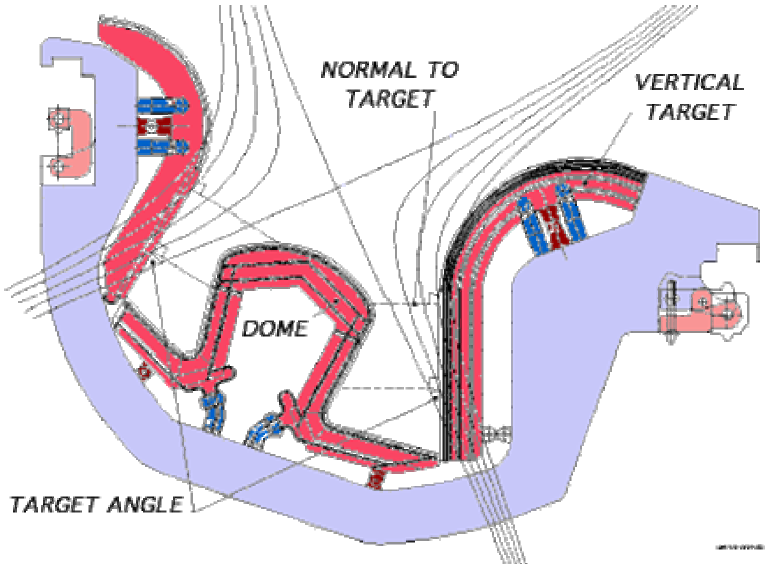

Divertor Target Power Deposition: IR, TC, LP

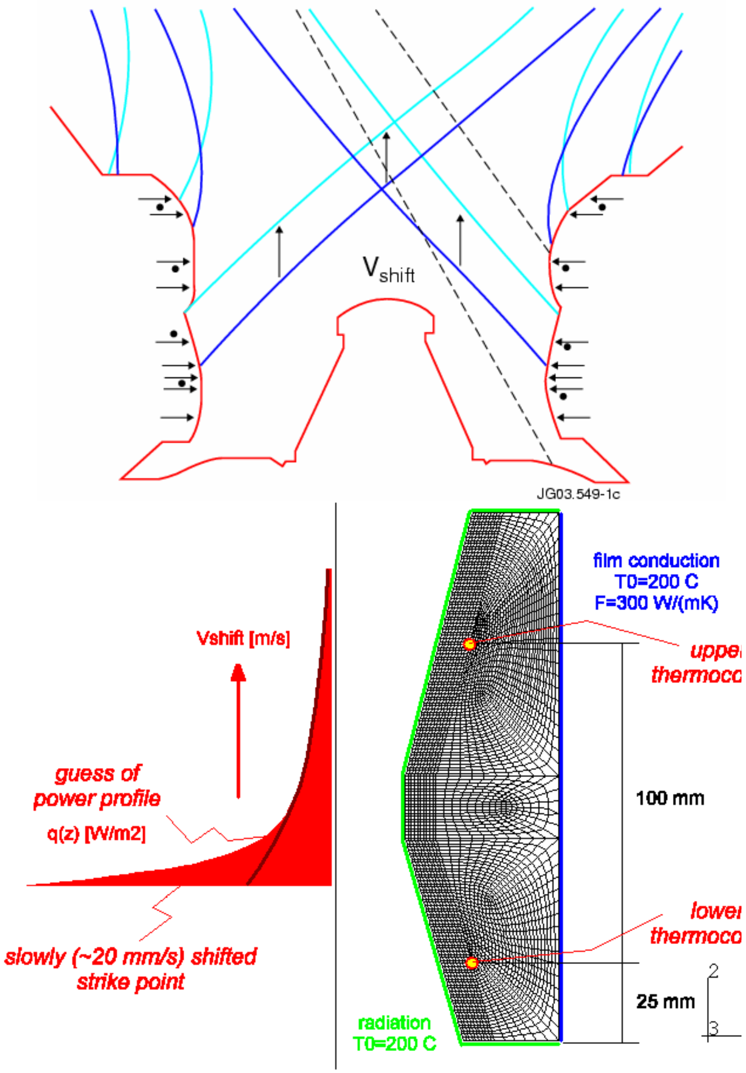

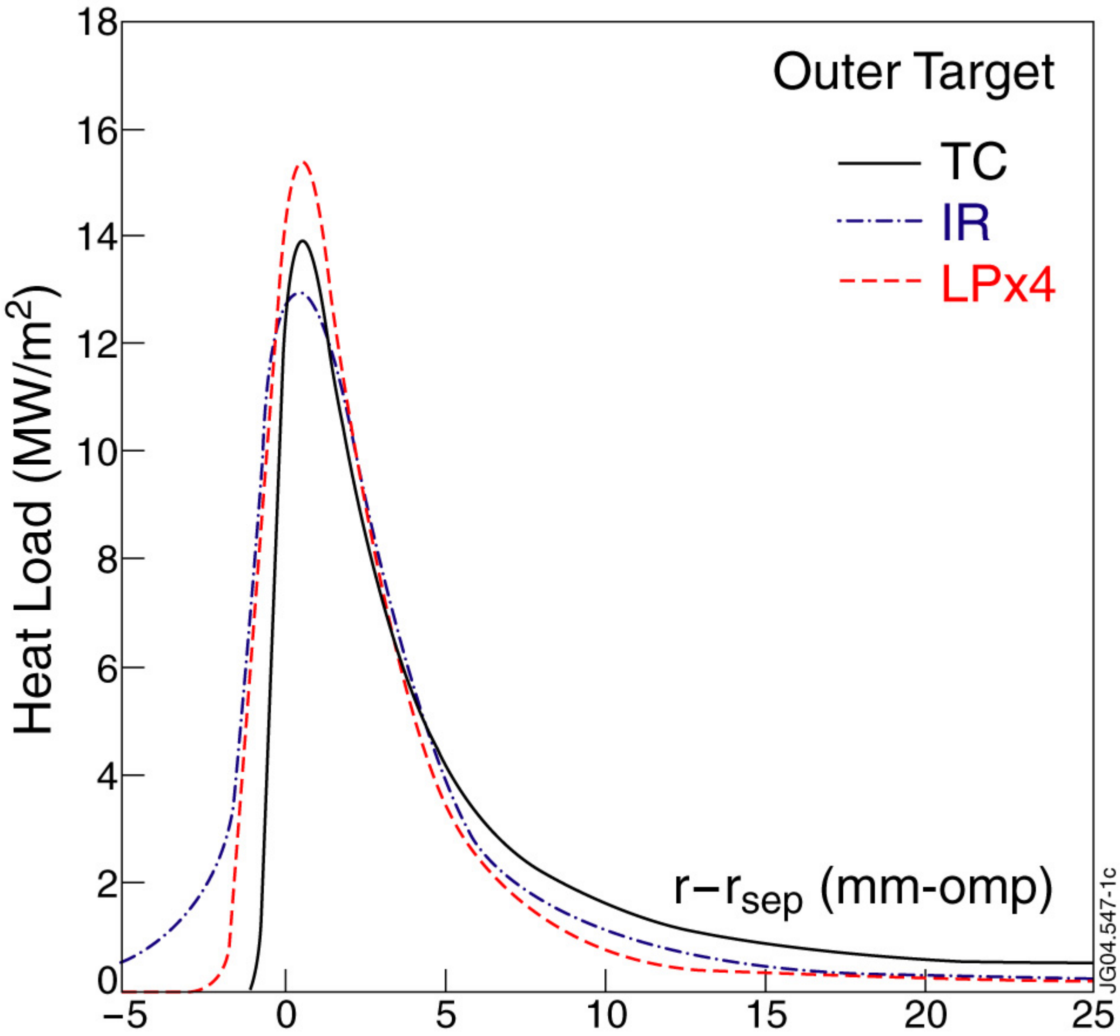

Forward field (fwd-B) ELMy H-modes: B×∇B↓

$$\lambda_q^H \propto A(Z)^{1.1\pm0.12}\, B_\phi^{-0.93\pm0.2}\, q_{95}^{0.41\pm0.27}\, P_{div}^{-0.48\pm0.09}\, n_e^{0.15\pm0.13}$$

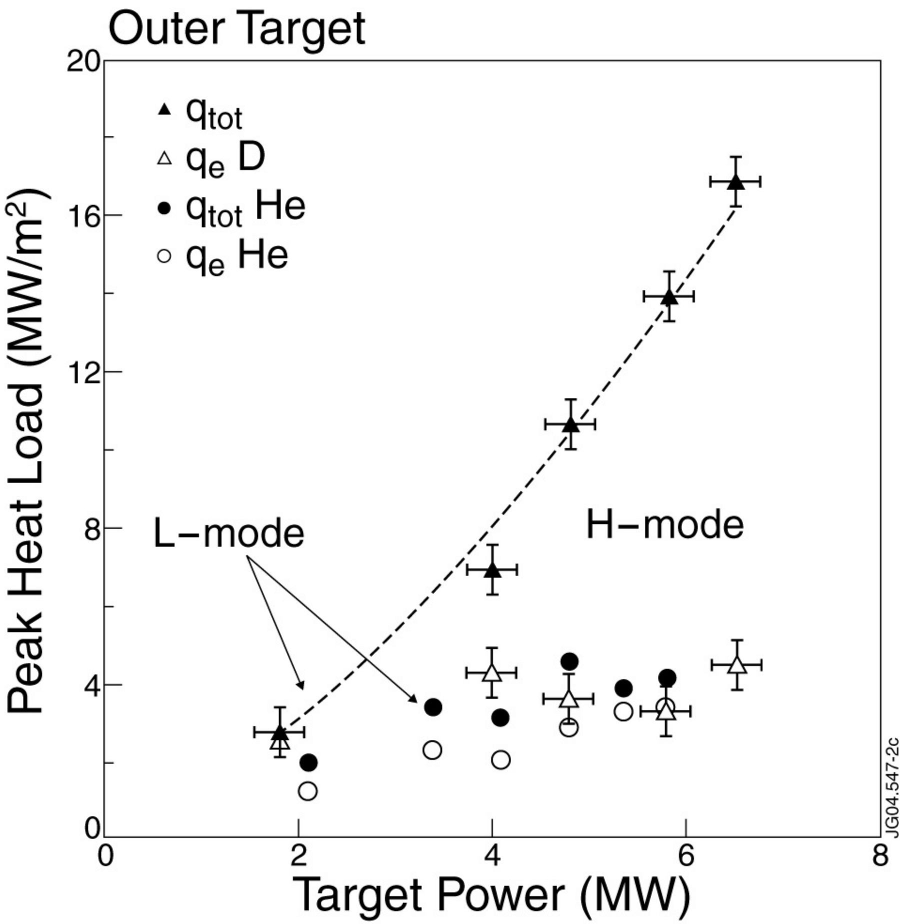

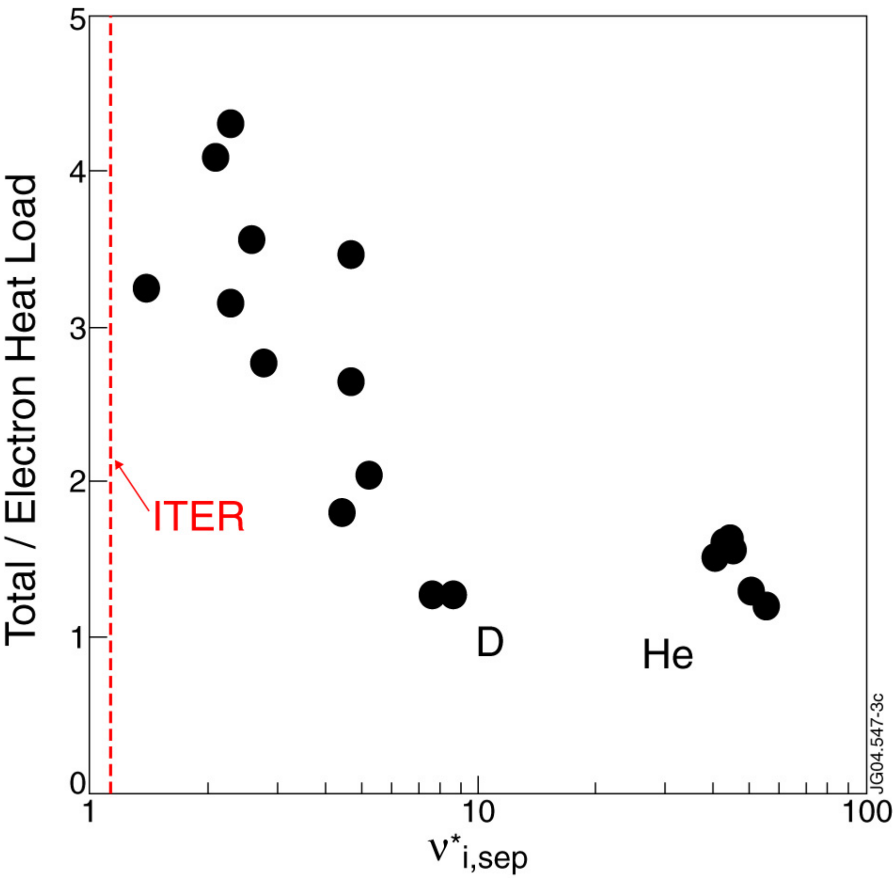

Comparison with theories of ⊥ SOL energy transport

$$\lambda_q^H \propto A(Z)^{1.1\pm0.12}\, B_\phi^{-0.93\pm0.2}\, q_{95}^{0.41\pm0.27}\, P_{div}^{-0.48\pm0.09}\, n_e^{0.15\pm0.13}$$

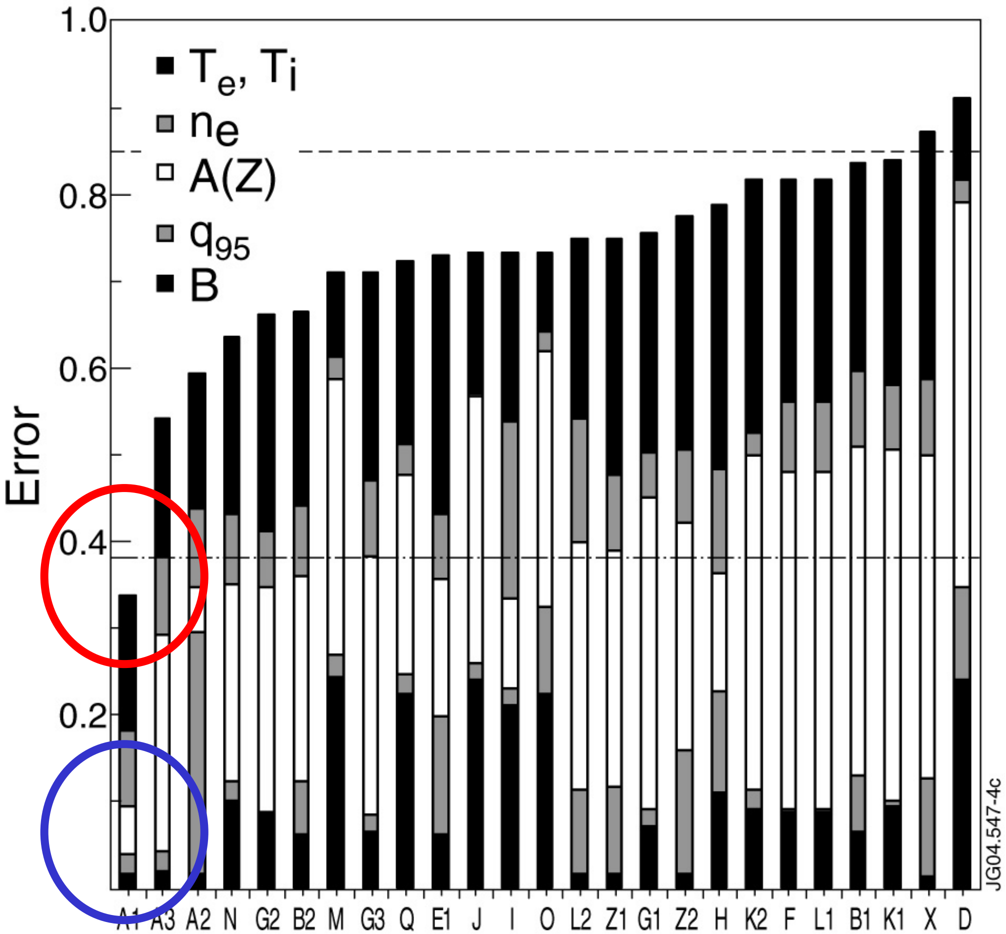

Scaling and **Magnitude** consistent with classical ion conduction

$$\lambda_q \sim 2.25\, \lambda_q^{\mathbf{A1}} \sim 0.27\, \lambda_q^{\mathbf{A2}}$$

$$\chi_\perp^{SOL} \sim (1\text{-}5)\, \chi_\perp^{A1}$$

as well as collisionally modified ion orbit loss

$$\lambda_q \sim 2.4\zeta\lambda_q^{\mathbf{A1}} + (1-\zeta)\lambda_q^{\mathbf{IOL}},$$

$$\zeta = \nu^*_i / (1 + \nu^*_i)$$

Ion orbit loss (ASCOT) profiles: fwd-B vs. rev-B

Very sensitive to field reversal; outer profile broadened

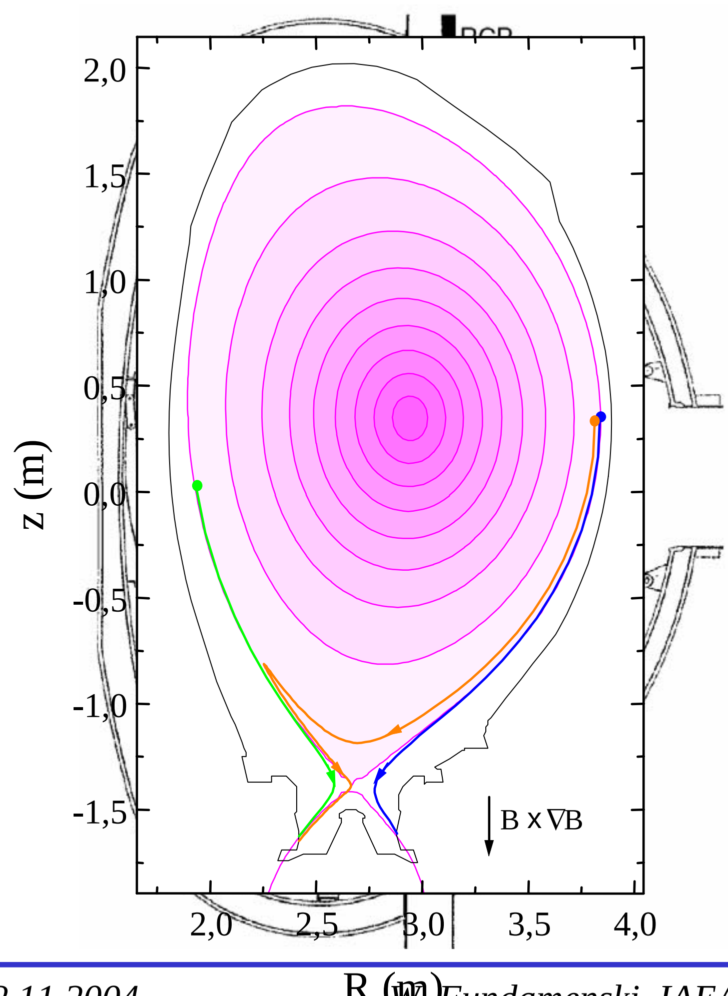

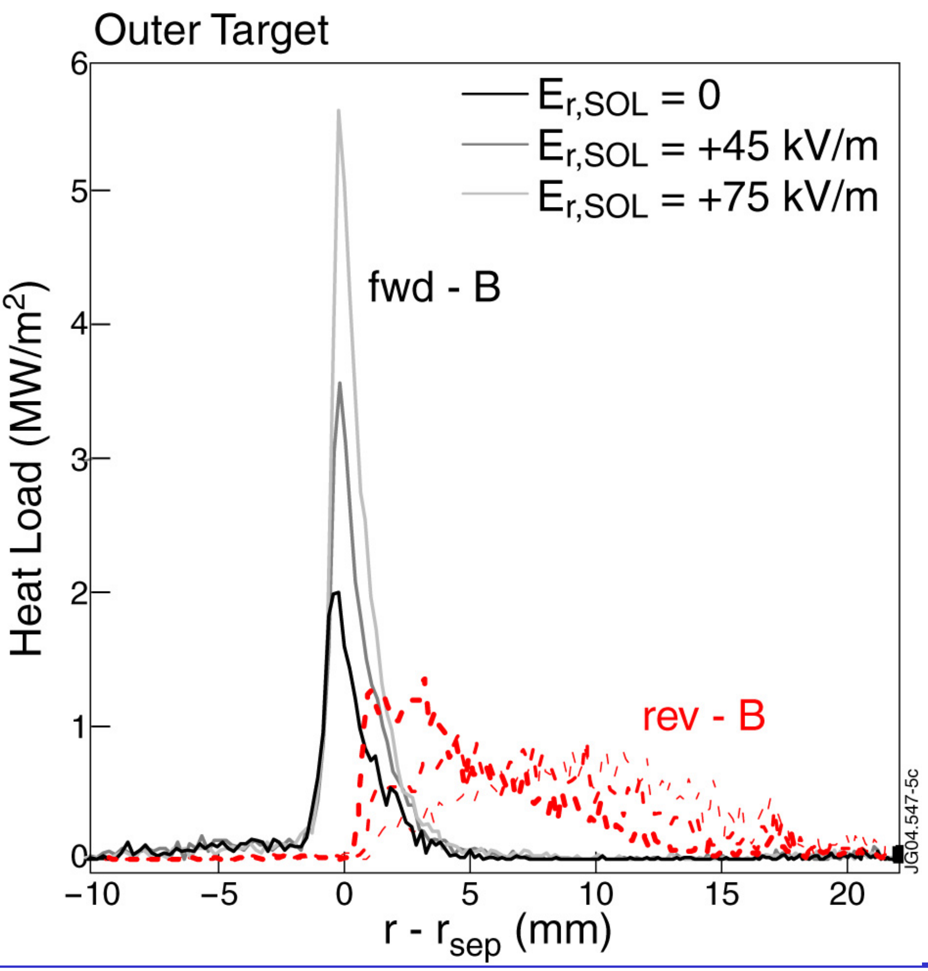

Reversed field (rev-B) ELMy H-modes: B×∇B↑

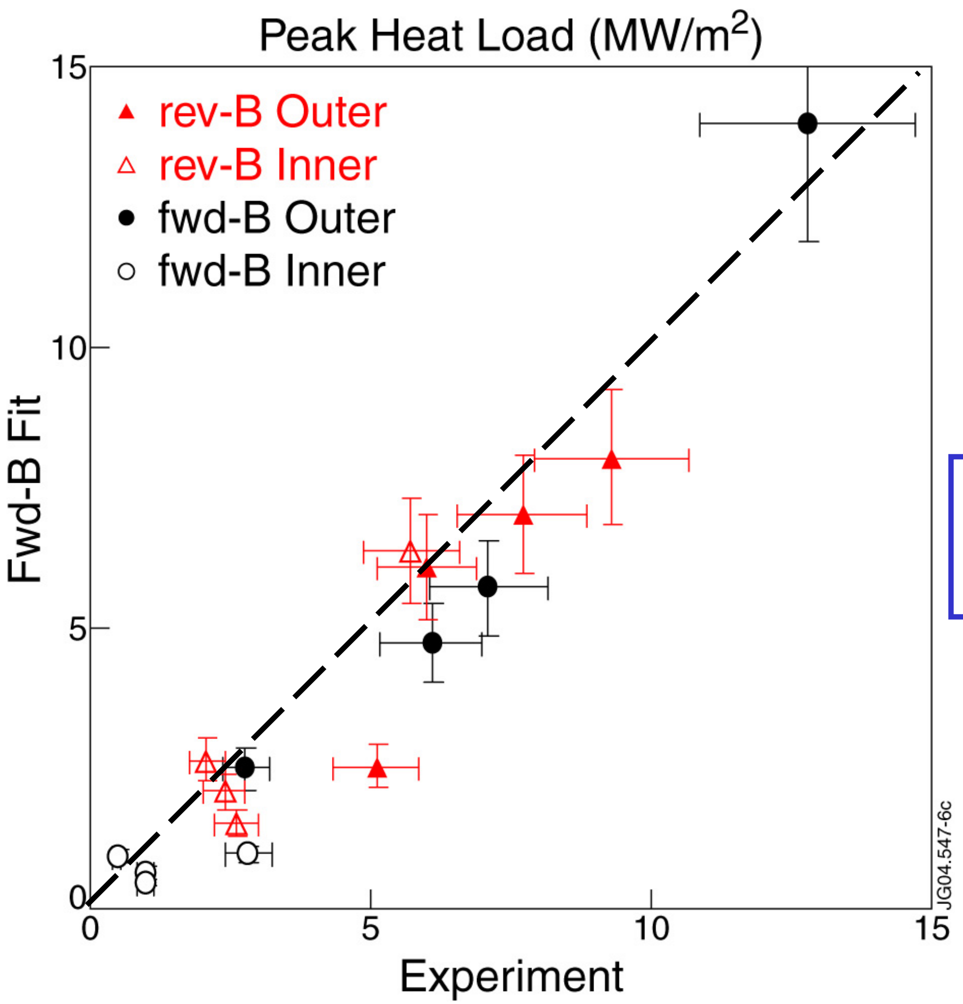

Rev-B peak heat flux well matched by **fwd-B** scaling

∴Radial profiles and transport, insensitive to B×∇B direction !

Consistent with neo-classical ion conduction, but **not** ion orbit loss!

ITER prediction: $\lambda_q^{TC} \sim 3.7 \pm 1.1$ mm at entrance to divertor volume

ELM power exhaust experiments

$$\Delta t_{||} \sim 125 \pm 70\ \mu s \sim \tau_{||} \sim L_{||} / c_{s,ped}$$

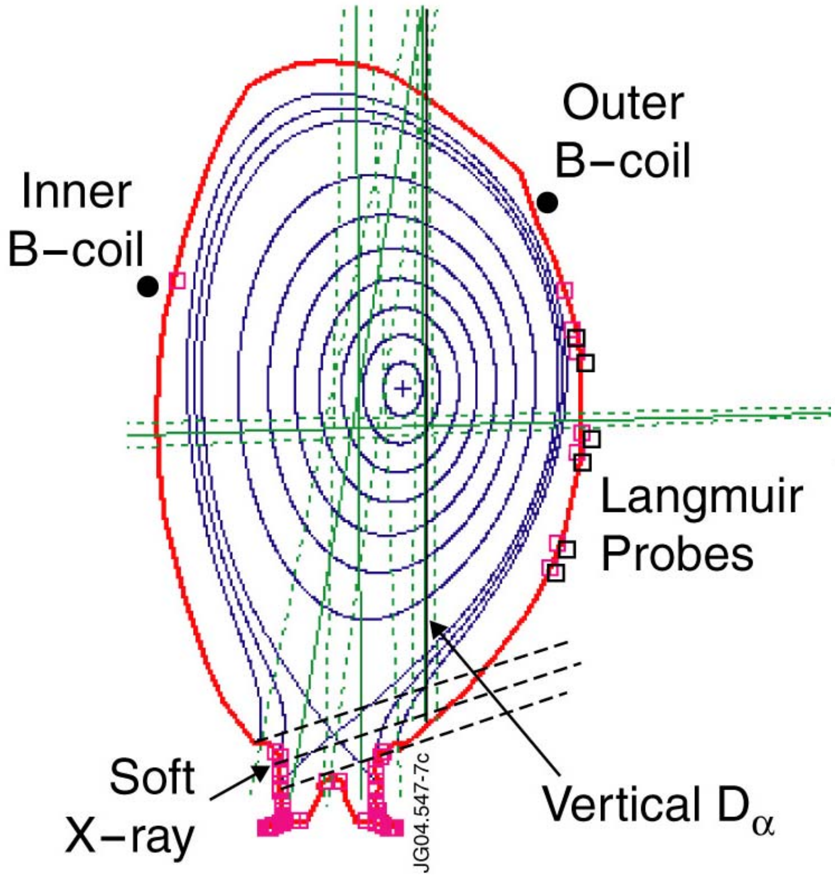

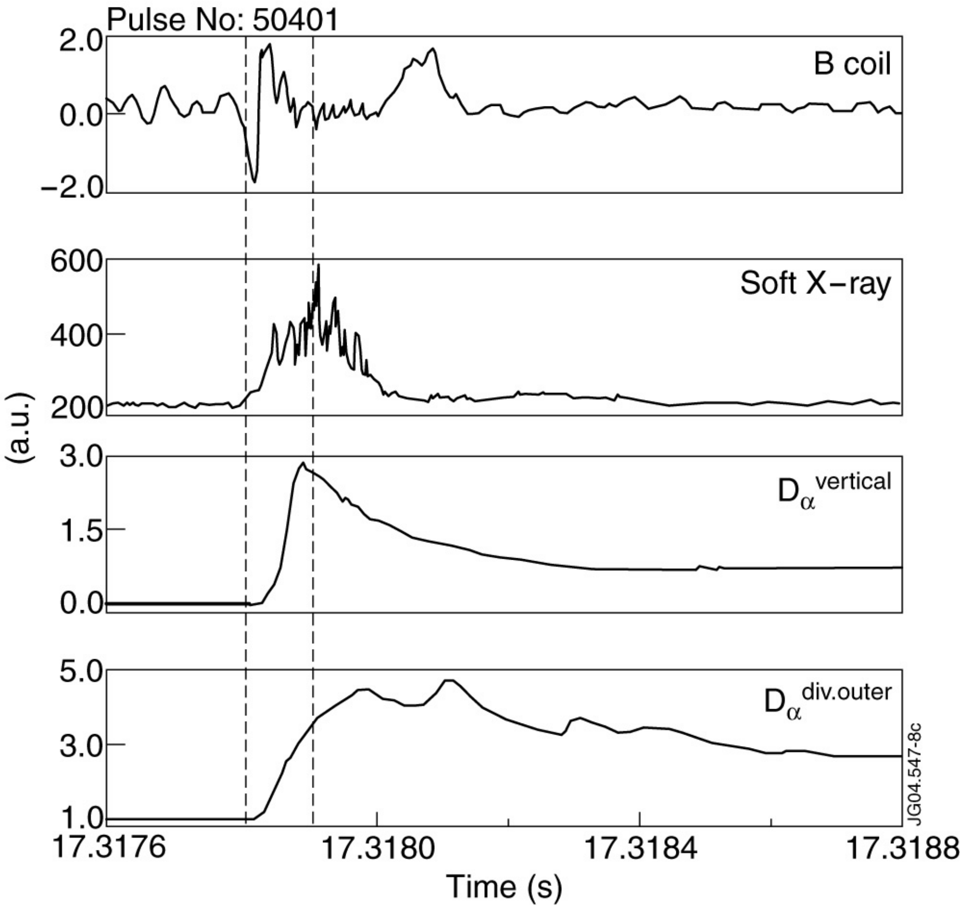

Advective-diffusive radial ELM propagation

$$G(t,r) = \frac{A}{\sqrt{D_\perp t}} \exp\left(-\frac{(r - v_\perp t)^2}{D_\perp t} - \frac{t}{\tau_{||}} \right)$$

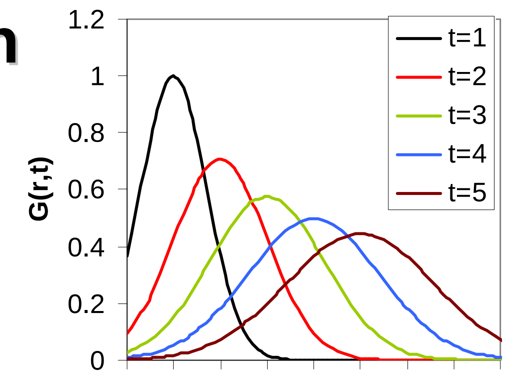

$\langle v_\perp \rangle \sim r_{lim} / \tau_\perp \sim 450 - 750$ m/s

$\langle v_\perp \rangle / \langle c_s \rangle \sim 0.25 - 0.4$ %

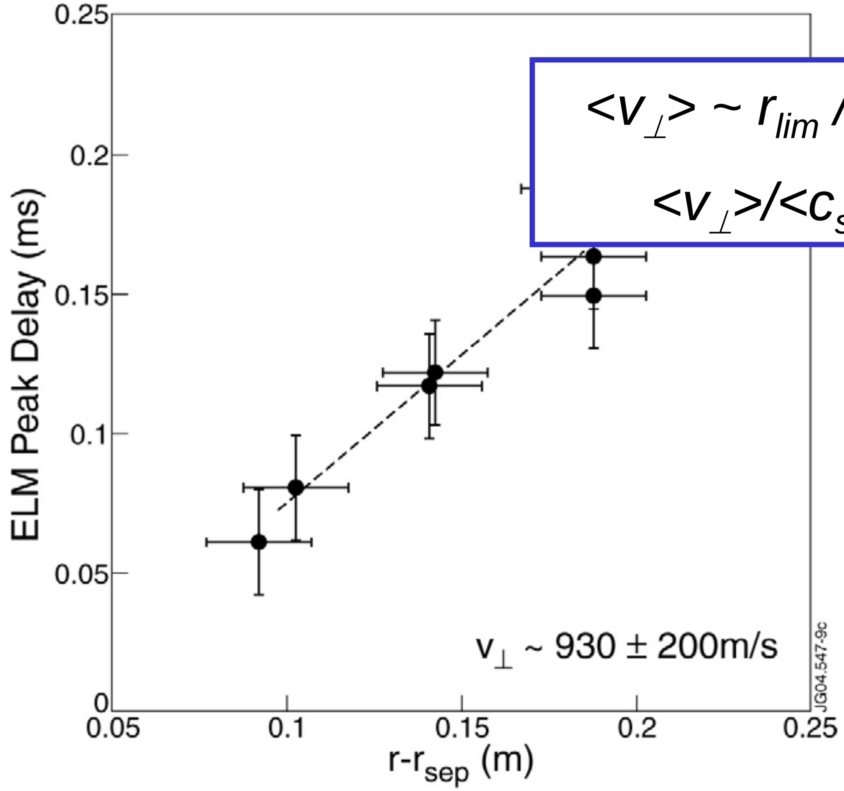

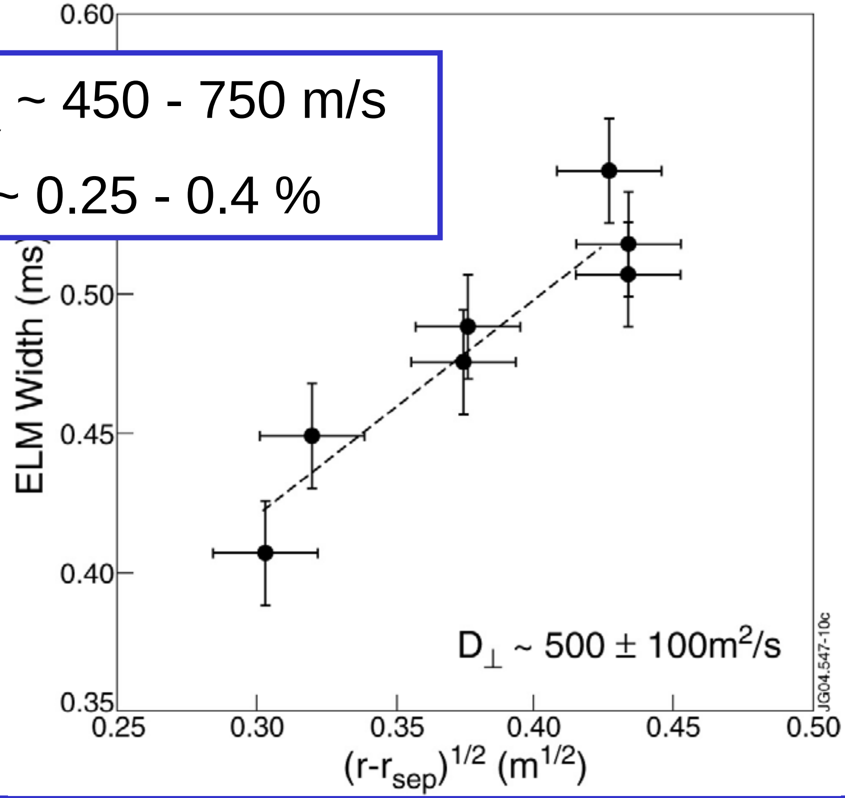

Comparison with theory: plasmoid propagation model

$\perp$ drive mechanism = sheath resistivity, curvature and E×B drifts

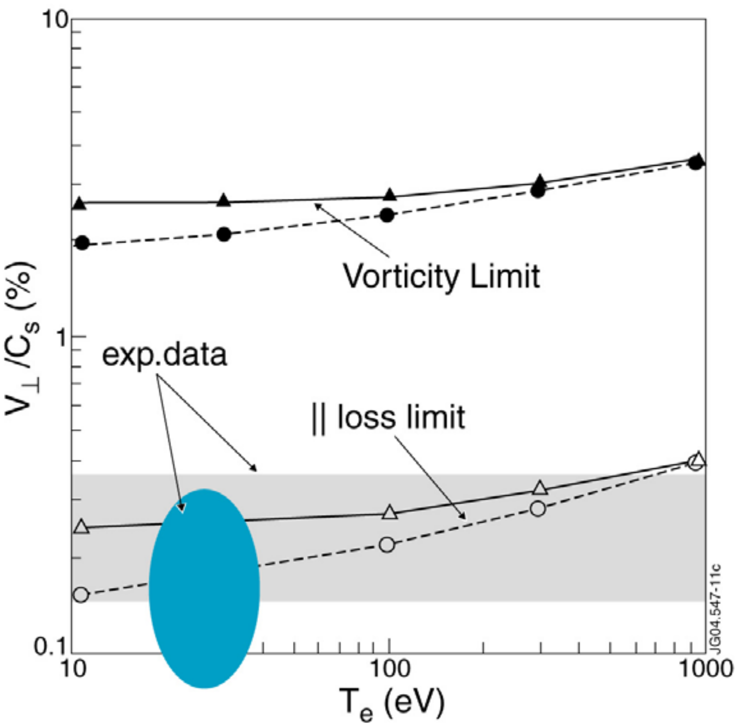

ELM values:

$\delta_\theta \sim \delta_r < 10$ cm

$\lambda_n < 12$ cm

$T_{e,lim} \sim 25$ eV

$T_{i,lim} > 75$ eV

$\lambda_{Te} < 3$ cm

$\lambda_{Ti} < 8$ cm

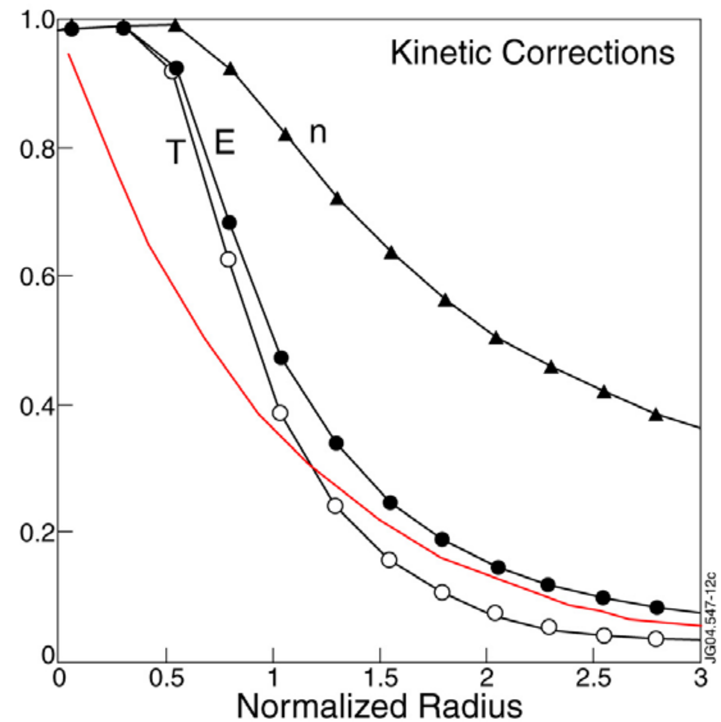

ITER limiter load: $\lambda_{Te} < 3$ cm, $\lambda_{Ti} < 6$ cm with $r_{lim} = 5$ cm

$n_e < 3.0\text{x}10^{19}$ m^{-3}, $T_i \sim 2.5T_e < 1.0 \pm 0.2$ keV

EURATOM - IPP Association,
Garching, Germany

Wall and Divertor Load during ELMy H-mode and Disruptions in ASDEX Upgrade

A. Herrmann, **J. Neuhauser, G. Pautasso, V. Bobkov, R. Dux, T. Eich, C.J. Fuchs, O. Gruber, C. Maggi, H.W. Müller, V. Rohde, M. Y. Ye, ASDEX Upgrade team**

Presented by W. Fundamenski

Global power balance within 20 %

but power on main chamber due to hot spots, ELMs and Disruptions

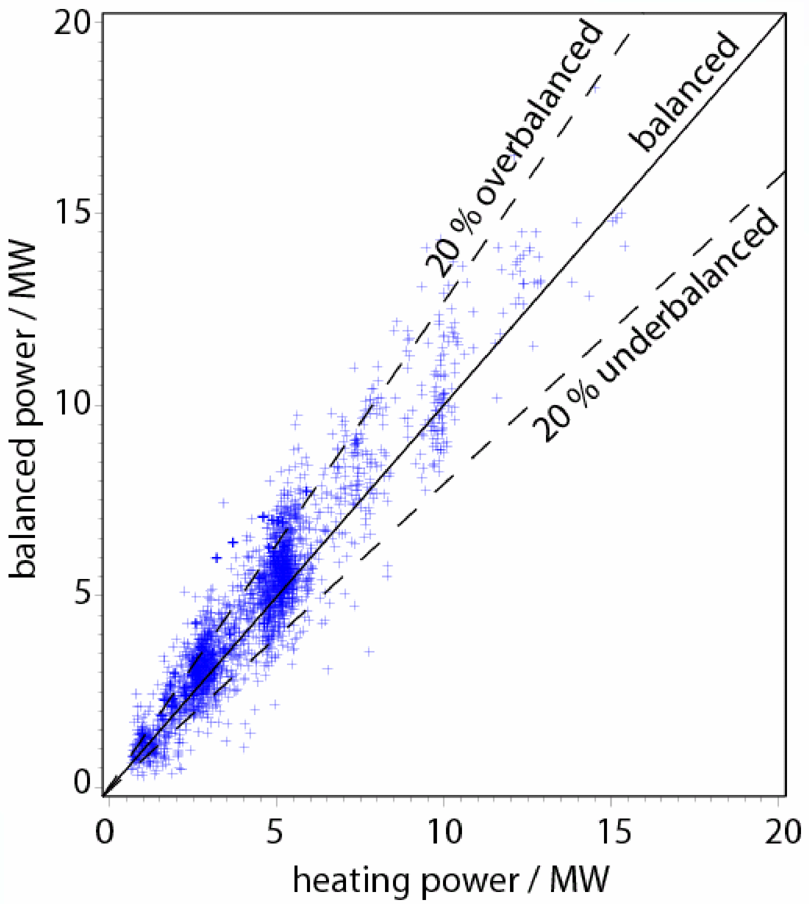

25% of ELM energy to main chamber wall

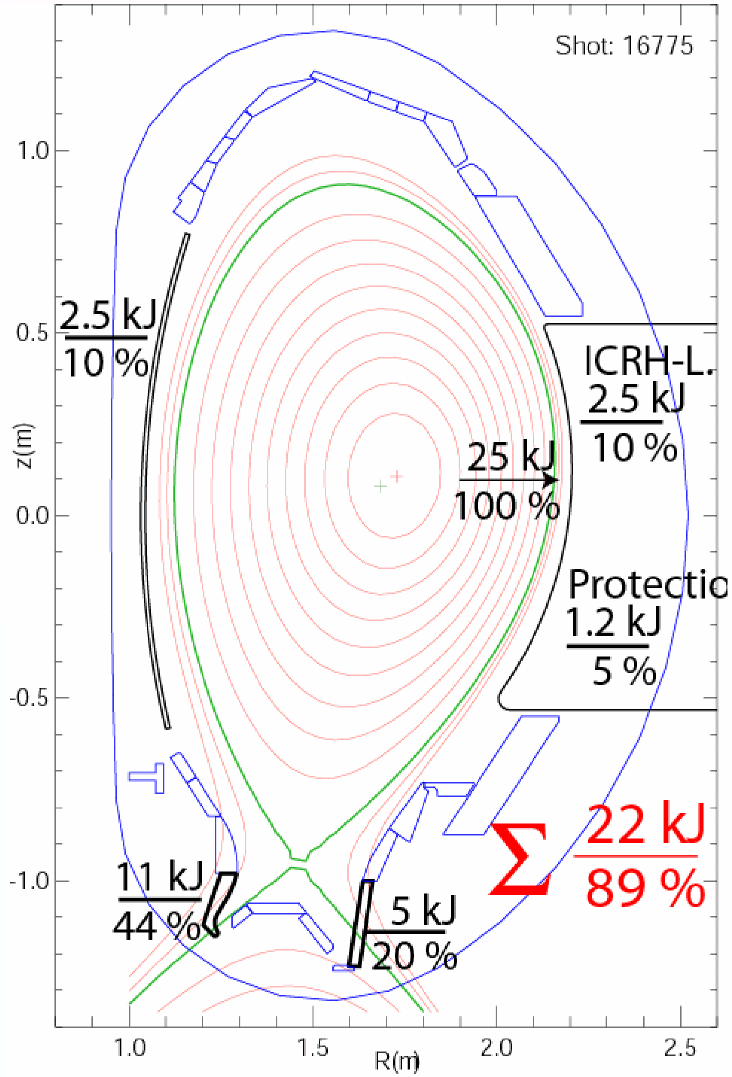

- fair power balance at ~ 90%
- measured by IR
- calibrated by TC and calorimetry
- 10% of ELM energy to inner wall
- 15% of ELM energy to outer wall
- ELM radiation ?

A. Herrmann, PPCF 46(2004)971

10 to 40 % of ELM energy radiated

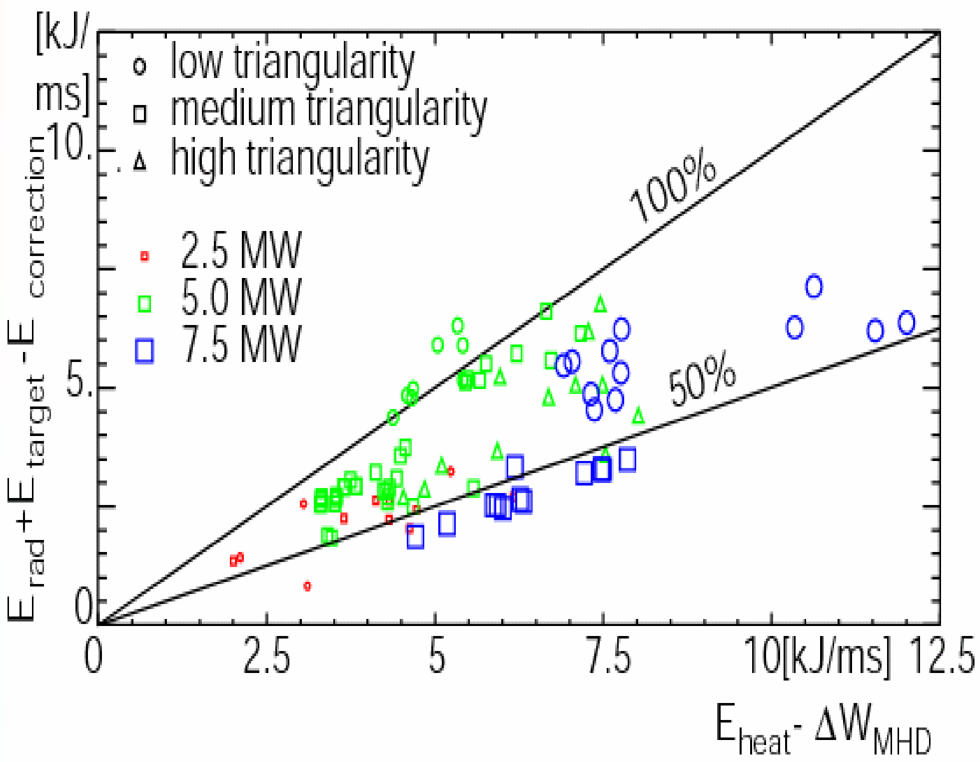

- Mostly in inner divertor
- Independent of ELM size and density
- reduction with triangularity
- tendency to be overbalanced

J.C. Fuchs, PSI 2004

Test limiter probe measures ELM power profile

separatrix moved from 2.5 cm to 6.5 cm away from the limiter

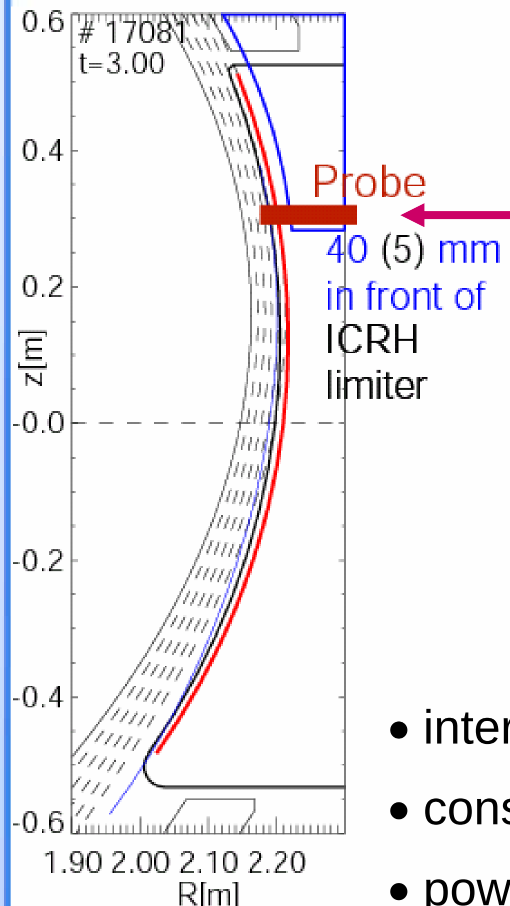

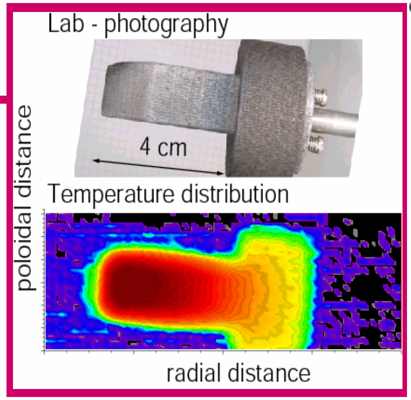

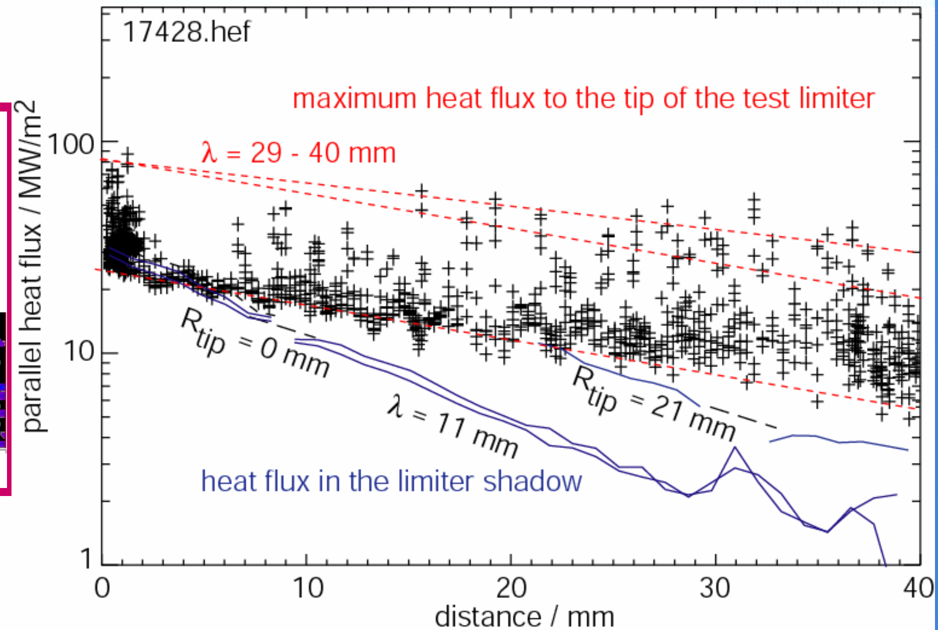

- inter-ELM and ELM power decay lengths in the SOL ~ 3-4 cm
- consistent with $v_\perp/c_s$ ~ constant, for turbulent eddies and ELMs
- power decay lengths in the limiter shadow ~ 1-2 cm

A. Herrmann, PPCF 46(2004)971

Helical ELM filaments observed

on upper outer divertor and outboard limiter

- Stripe energy content << 1% of total
- v_{tor}^{ELM} ~ 350 Hz << 3.5 kHz ~ $v_{tor}^{inter\text{-}ELM}$

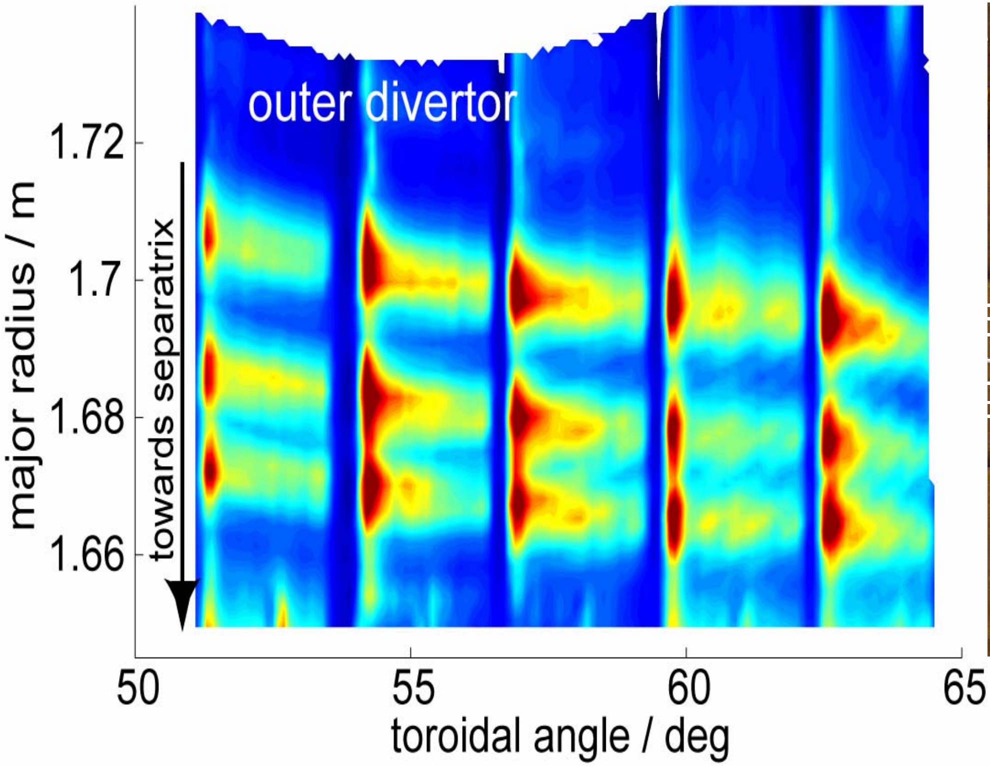

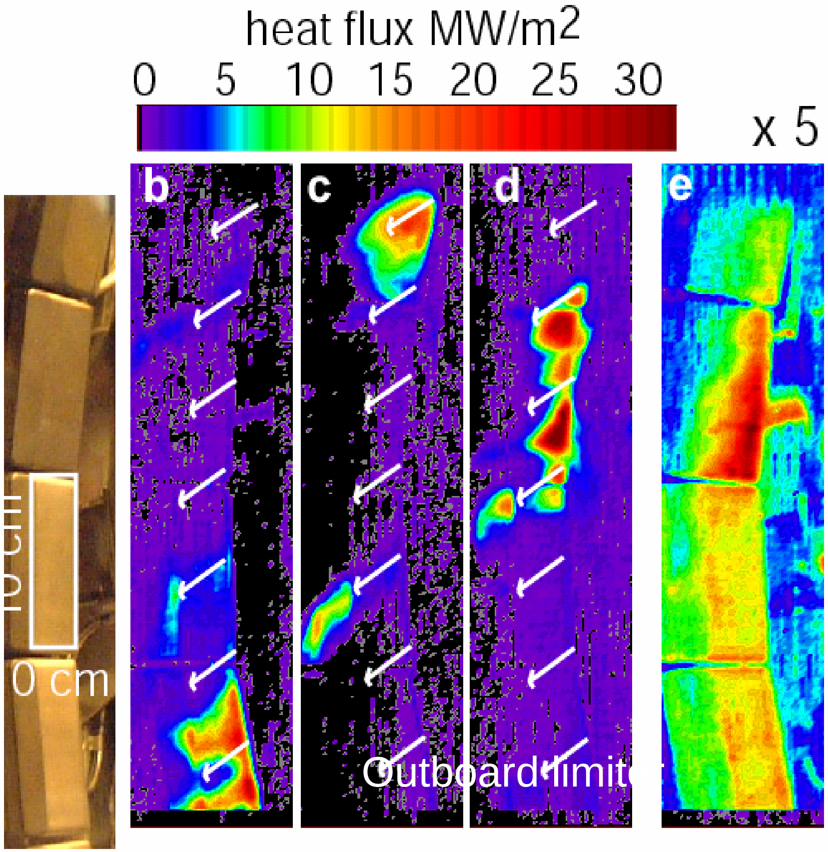

T. Eich, Physical Review Letters, **91** (2003)

Disruption heat load to main chamber wall

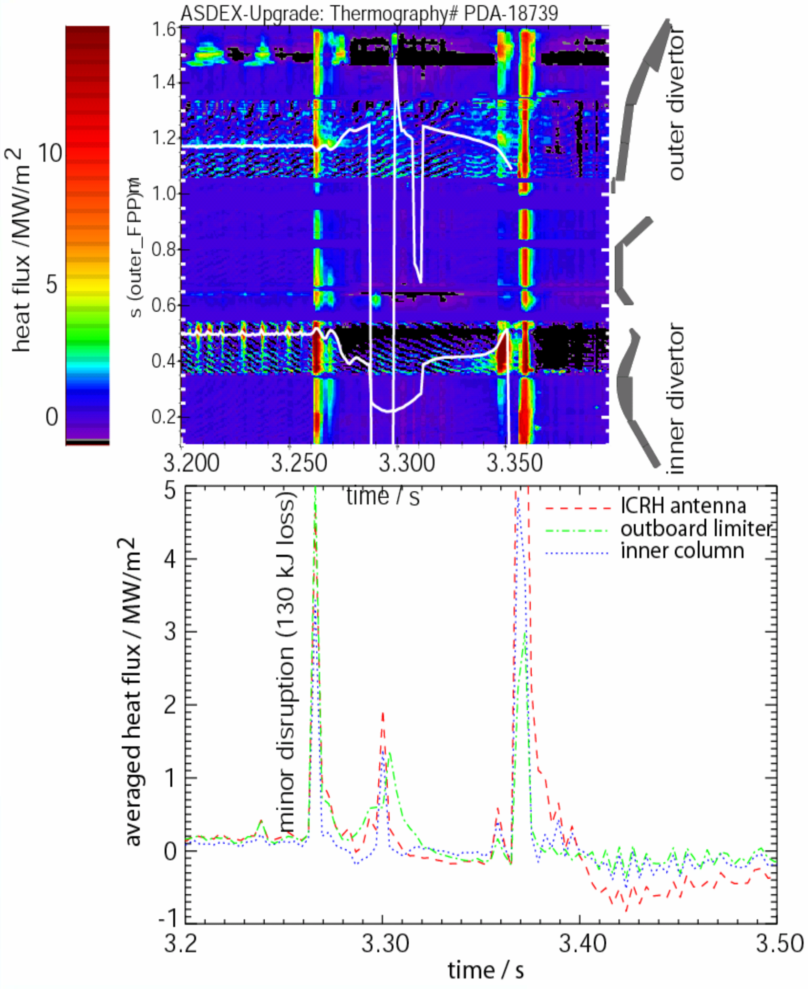

- density limit disruption
- ~ 90% lost in thermal quench phase
- heat deposition
  - fast rise: 0.1-0.5 ms
  - duration: few ms
- strong broadening on target
- significant power to non-divertor components.

See A. Loarte, this conference

Conclusions (JET and AUG):

- Steady state, Type-I ELMy H-mode radial power exhaust on JET dominated by weakly collisional ions
  - experimental data well matched by neo-classical ion conduction
  - predicts tolerable divertor heat loads for ITER
- Helical ELM structure observed on AUG
- Type-I ELM radial velocity agrees with sheath limited model (JET)
- ELM power decay length comparable to outer gap on JET and AUG
  - could pose problems for beryllium limiter on ITER
- Broad footprint (divertor and first wall) of heat flux deposition during disruption observed on AUG

Power Exhaust Summary:

<table>
<tr><th></th><th></th><th>AUG</th><th>JET</th><th>ITER</th></tr>
<tr><td rowspan="2">Steady state (inter-ELM)</td><td>Electron</td><td colspan="3">Interchange & drift wave turbulence</td></tr>
<tr><td>Total</td><td>–</td><td>(neo-)classical ion conduction</td><td>$\lambda_q \sim 4$ mm</td></tr>
<tr><td rowspan="2">Transient (intermittent eddies, ELMs)</td><td>Electron</td><td>$\lambda_{qe}/R \sim 2$ %</td><td>$\lambda_{qe}/R \sim 1$ %</td><td>$\lambda_{qe} < 3$ cm</td></tr>
<tr><td>Total</td><td colspan="2">Advection-diffusion
$\lambda_q/R < 2$ %</td><td>$\lambda_q < 6$ cm</td></tr>
</table>

Characteristic times in the SOL

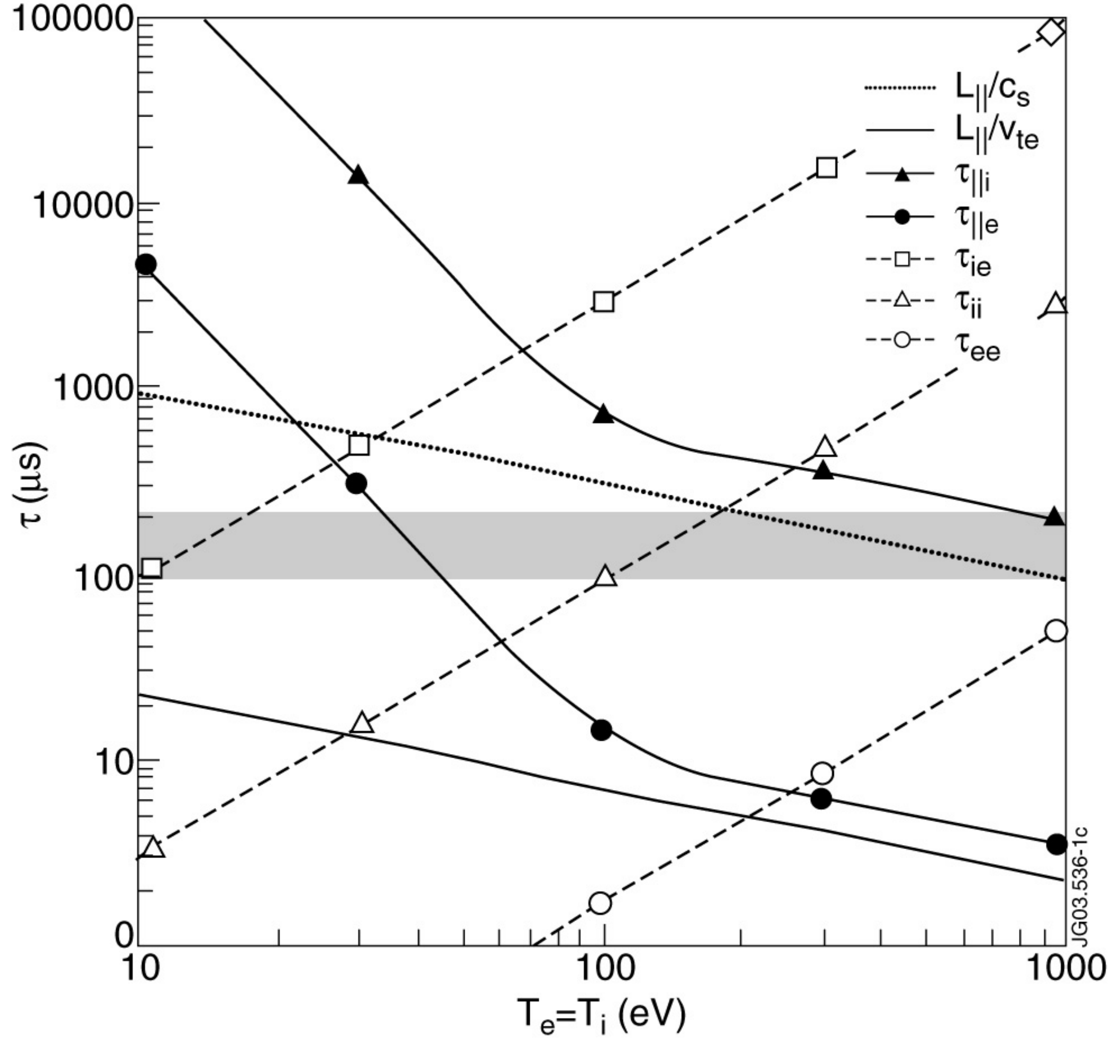

Kinetic estimates of || losses

$$\frac{N(r)}{N(0)} = \frac{\int_0^{v_{cr}} e^{-\beta v^2} dv}{\int_0^{\infty} e^{-\beta v^2} dv} = erf\left(\frac{\tau_{\|}}{\tau_{\perp}}\right) = erf\left(\xi^{-1}\right), \qquad 0 < \xi < 1$$

$$\frac{W(r)}{W(0)} = \frac{\int_0^{v_{cr}} v^2 e^{-\beta v^2} dv}{\int_0^{\infty} v^2 e^{-\beta v^2} dv} = erf\left(\xi^{-1}\right) - \frac{2}{\sqrt{\pi}} \xi^{-1} \exp\left(-\xi^{-2}\right), \quad 0 < \xi < 1$$

$$\xi \sim \frac{\tau_{\perp}}{\tau_{\|}} \sim 1, \qquad \xi_i \sim \frac{\tau_{\perp}}{\tau_{\| i}} \sim 1, \qquad \xi_e \sim \frac{\tau_{\perp}}{\tau_{\| e}} >> 1$$

Ratio of ion and electron dissipative scales in the SOL

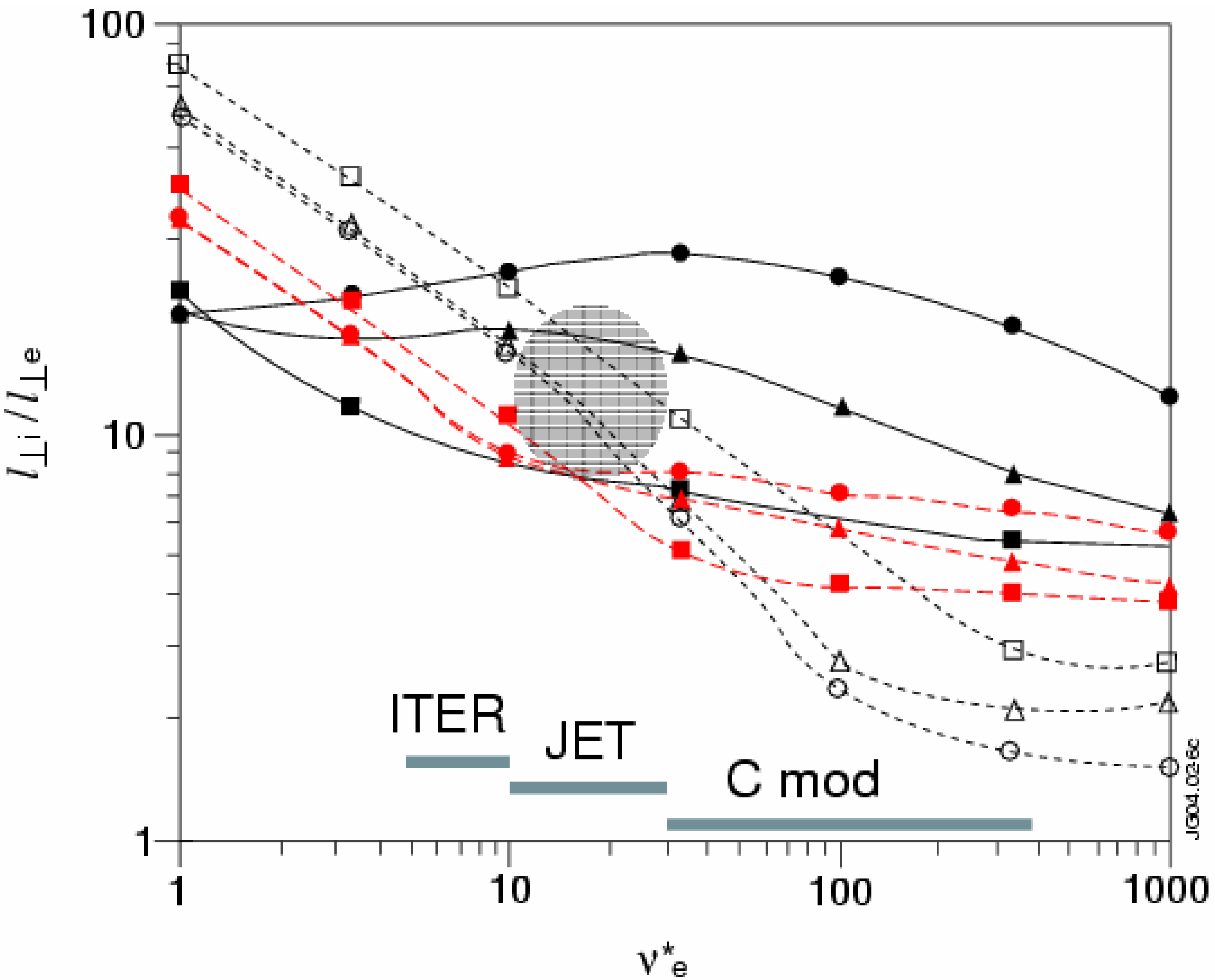

IR view into the vessel and the limiter positions

IR camera view

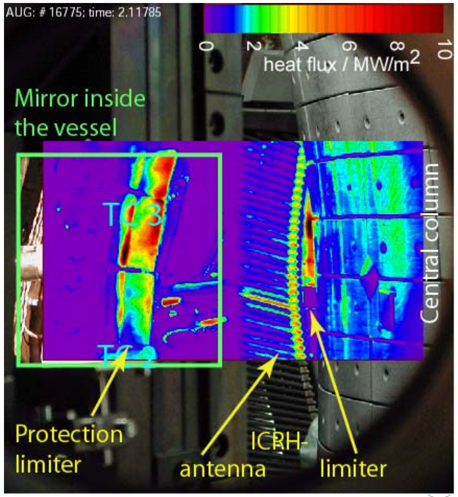

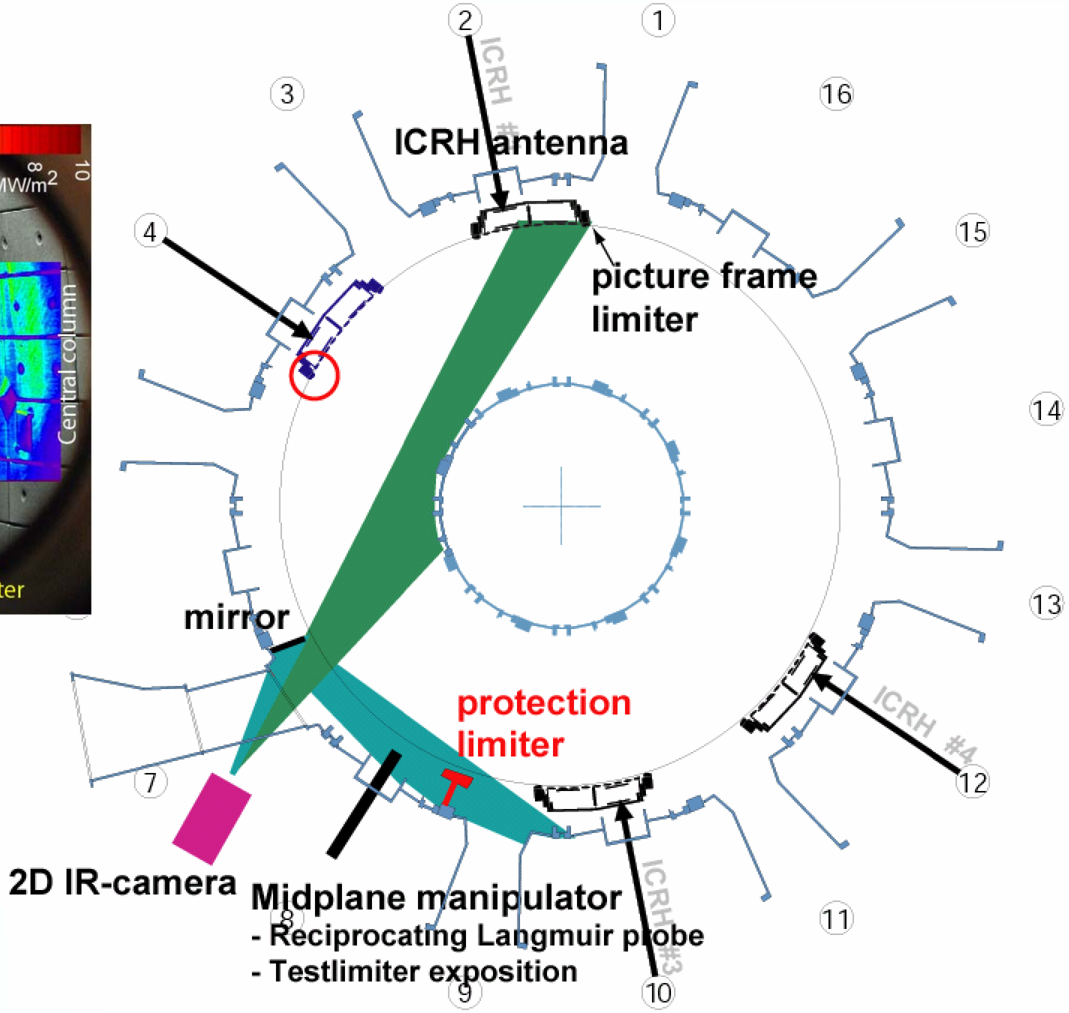

ELM ejected particles and energy partly deposited on limiters

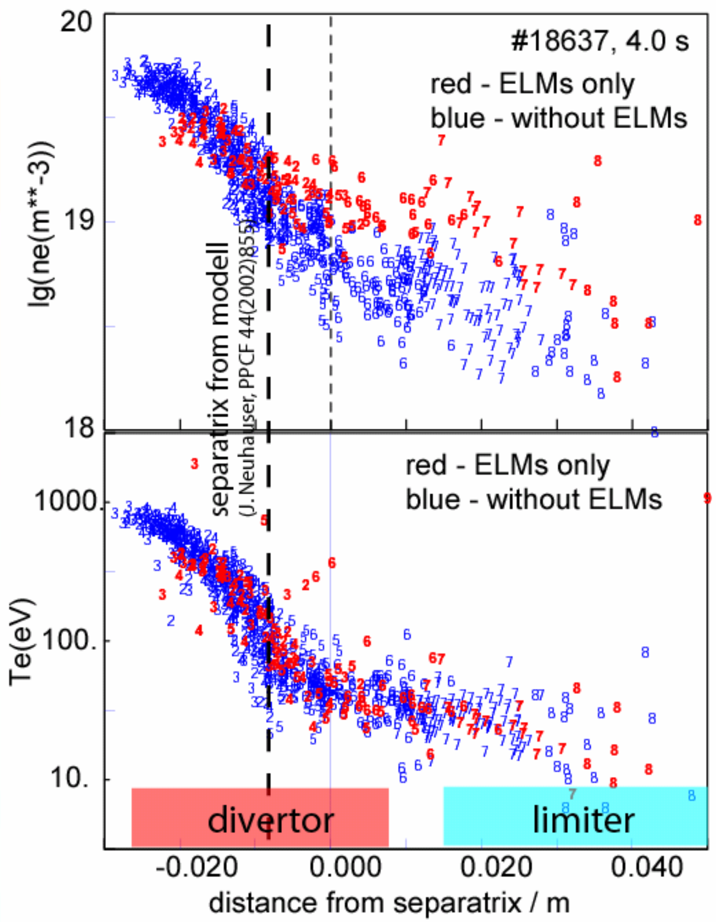

$\lambda(R) \approx$ 3-8 mm $\approx$ 30-80 mm

(3-7 mm in the limiter shadow)

Large variation of ELM signature remote from the separatrix.

ELM structure measured at the upper divertor.

T. Eich, *Physical Review Letters,* 91 **(2003)**

ELM resolving diagnostics for non divertor heat load

- Thermography
- Langmuir probes
- Test limiters (M.Y. Ye,PSI 2004)

Heat flux values at the far edge of the divertor and the leading edge of the limiter are consistent

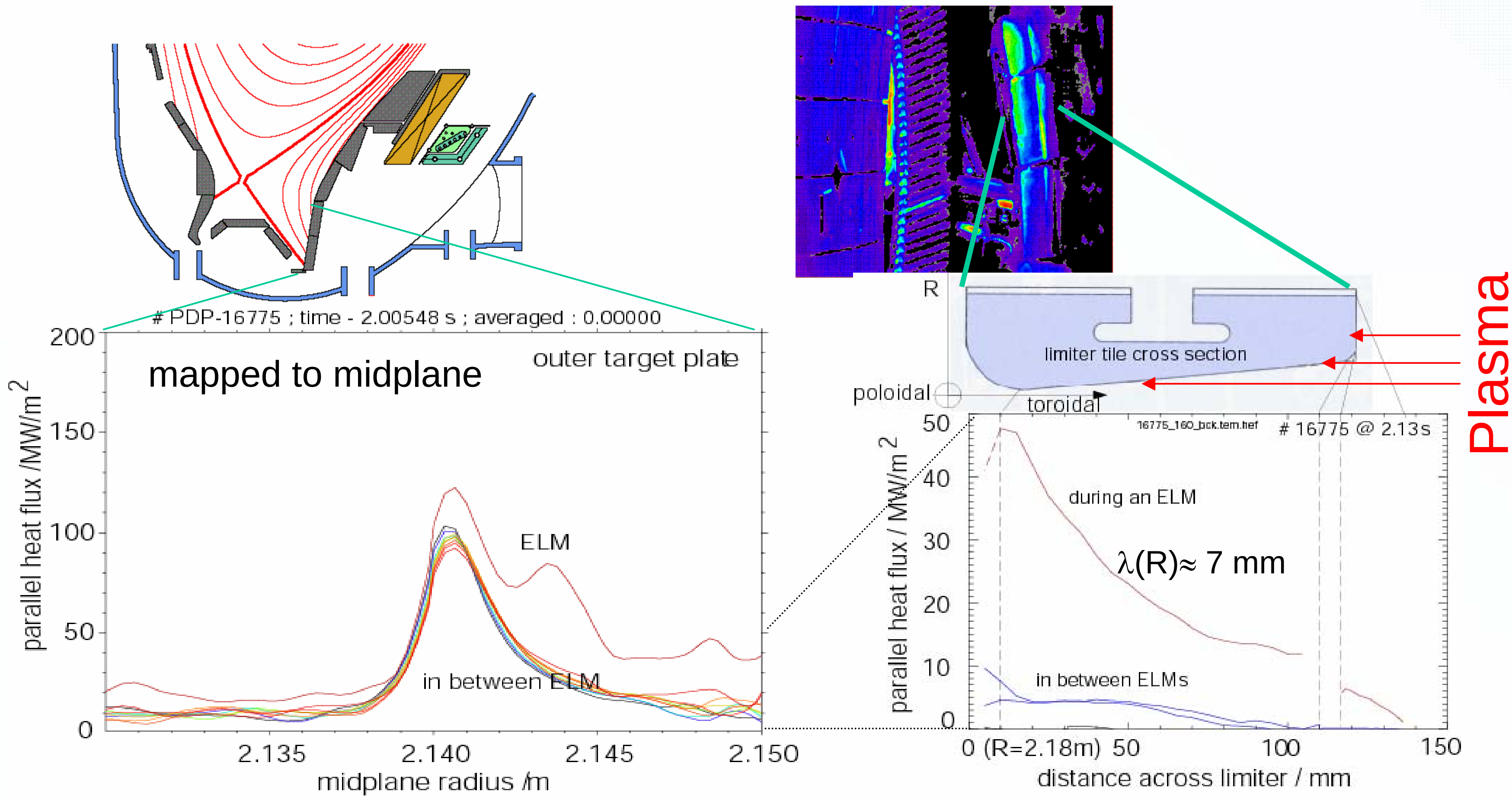

Experimental observation of local heat load is qualitatively understood

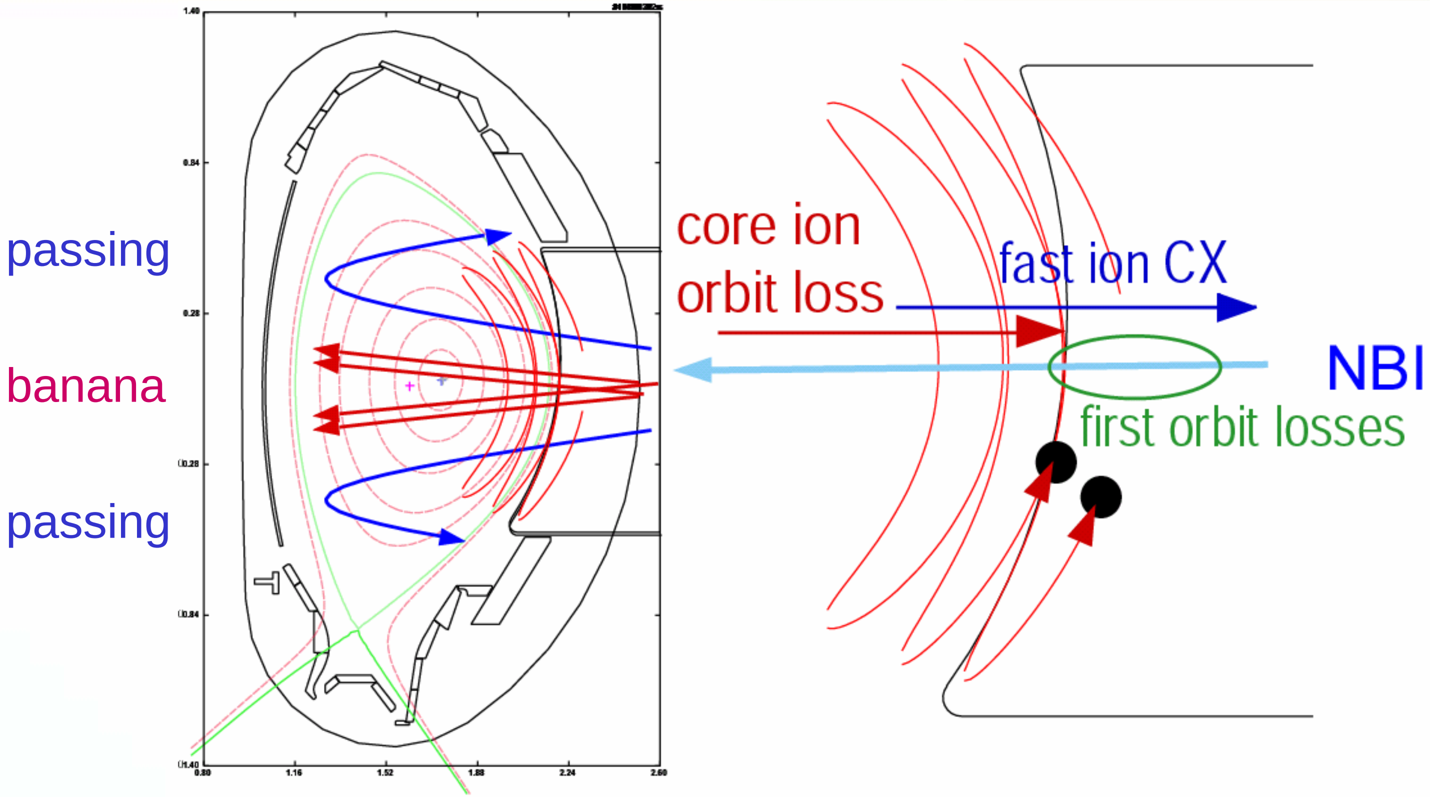

- Location of the intersection area depends on ionisation source location, magnetic field helicity, co/counter neutral injection and ...
- on non-axisymetric first wall structure.